Supplementary Information

A Tough and Stiff Ionogel Prepared by A Restricted Phase Separation Process

*Jinliang Xie[1], Xiaoqian Li[2], Zhongjie He[1], Ling Fan[3], Dongdong Yao[*1], Yaping Zheng[*1]*

[1] School of Chemistry and Chemical Engineering, Northwestern Polytechnical University Xi'an, Shaanxi 710072, P. R. China, Telephone and fax numbers: +86-029-88431688;

[2]Department of Ultrasonic Medicine, Tang Du Hospital, Air Force Medical University, No.569 of Xin Si Road, Xi'an, Shaanxi 710038. P. R. China;

[3] Guangxi Key Laboratory of Chemistry and Engineering of Forest Products, Guangxi Minzu University, Nanning 530006, P. R. China;

[*] Corresponding authors. E-mail: zhengyp@nwpu.edu.cn (Yaping Zheng), yaodd@nwpu.edu.cn (Dongdong Yao).

Table of Contents

Supplementary Note 1

The chemical structures of five ionic liquids were characterized by infrared-spectroscopy (Figure S2, Supplementary Information). The absorption peaks at 3279-3537 cm^{-1}, 3062 cm^{-1} and 1564 cm^{-1} were attributed to the ν(-C-H), ν(-CH=CH-) and ν(-C=N-) on the imidazole ring of [EBIM] cations, respectively. The sharp absorption peaks at 1468 cm^{-1} were attributed to the ν(-C-H) of methyl on the side chain of alkane, while the peak at 1690 cm^{-1} were attributed to the ν(-C=O) of TFA anions and the peak at 1059 cm^{-1} were attributed to the ν(B-F) of BF_4 anions, respectively. Combined with the results of FT-IR and ^{1}H-NMR (Supplementary Figure S1), it can be proved that all five ionic liquids have been successfully synthesized.

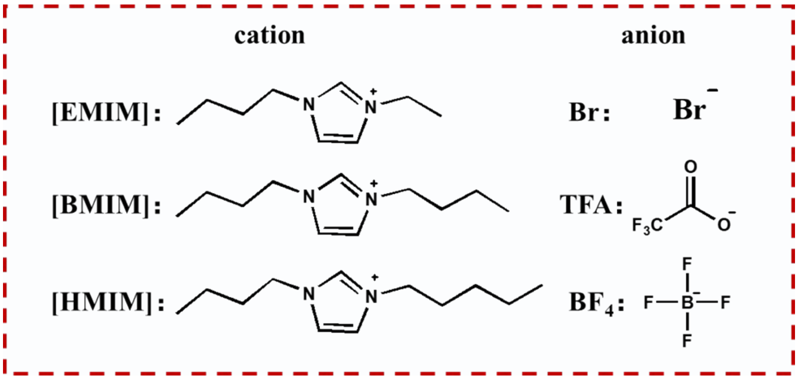

Figure S1. The cation and anion of ILs used in this work.

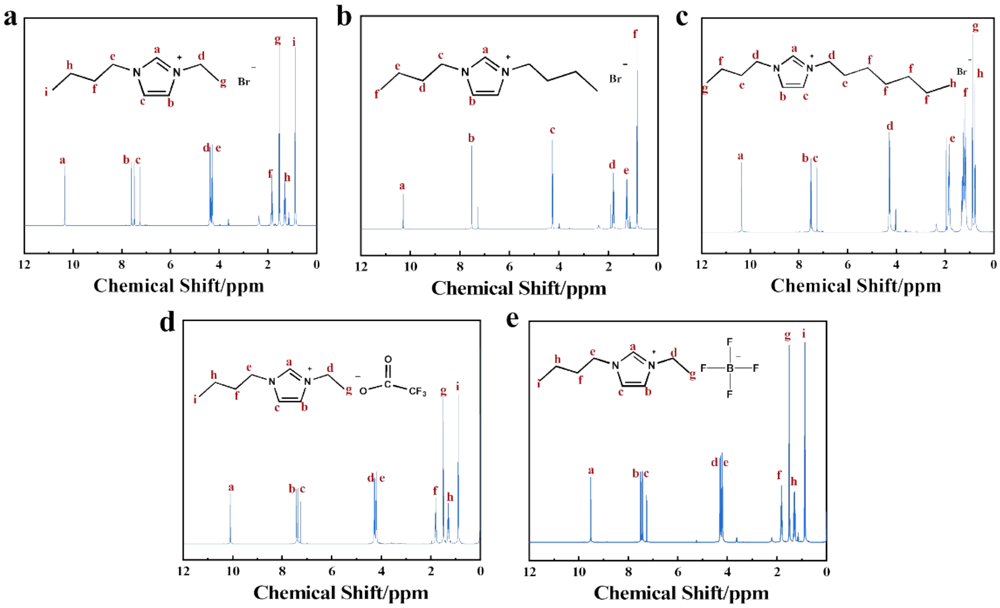

Figure S2. The [1]H-NMR spectra of ILs, (a) [EBIM]Br, (b) [BBIM]Br, (c) [HBIM]Br, (d) [EBIM]TFA, and (e) $[EBIM]BF_4$.

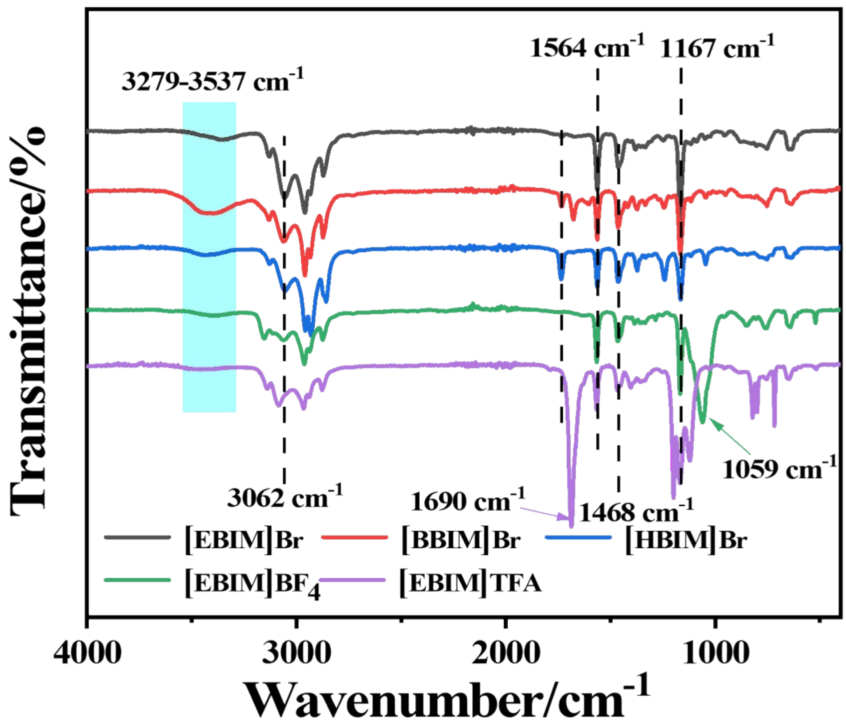

Figure S3. The FT-IR spectra of five kinds of ionic liquids.

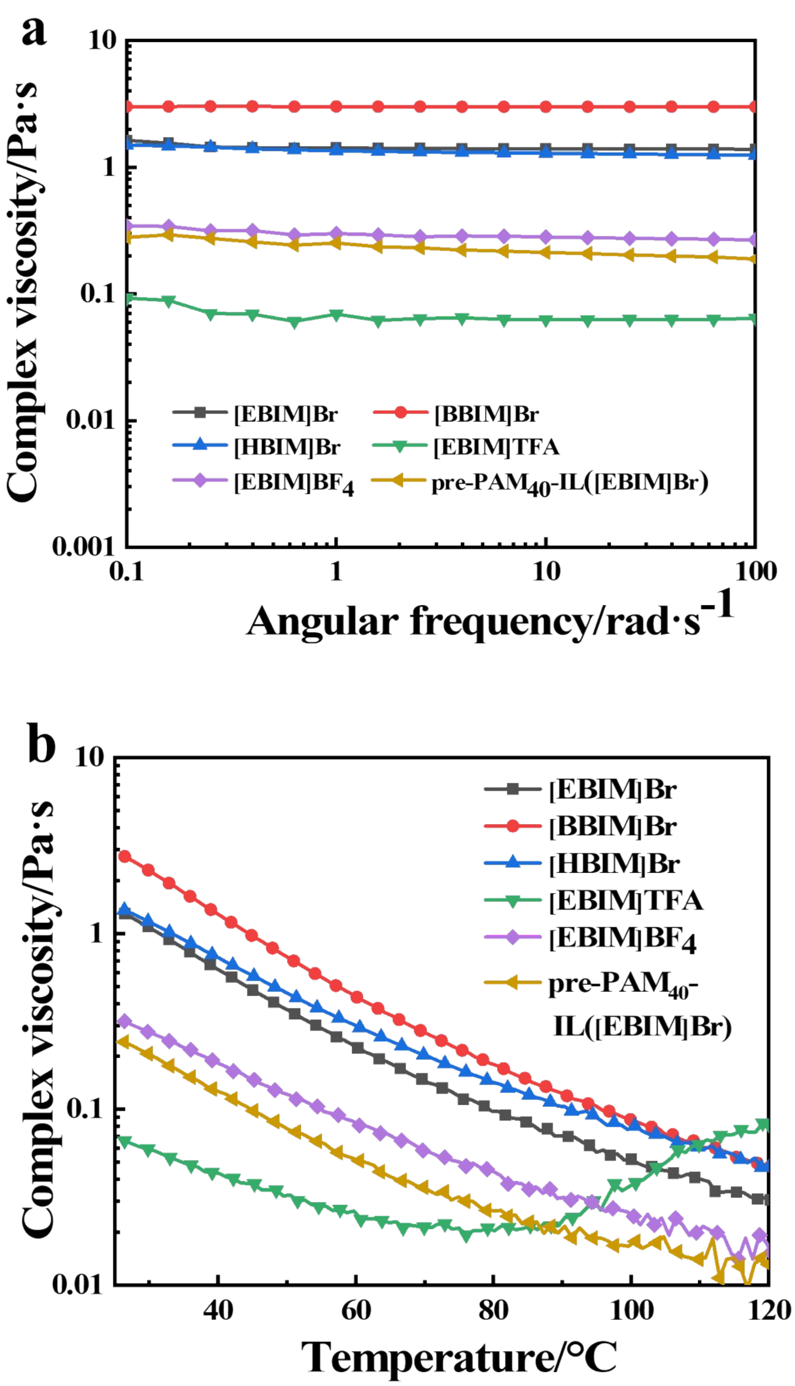

Figure S4. (a) The viscosity-frequency curves and (b) viscosity-temperature curves of five kinds of ionic liquids.

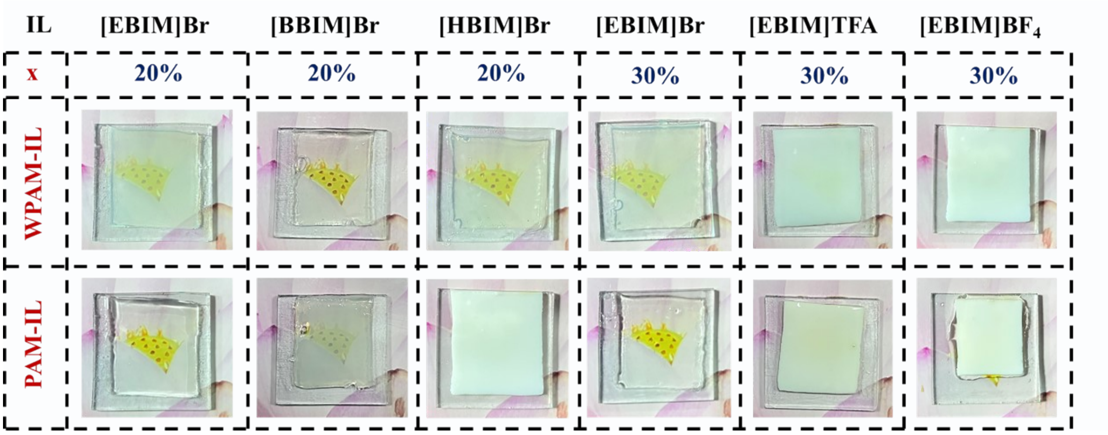

Figure S5. Optical photos of WPAM-IL and PAM-IL ionogels prepared with different ILs.

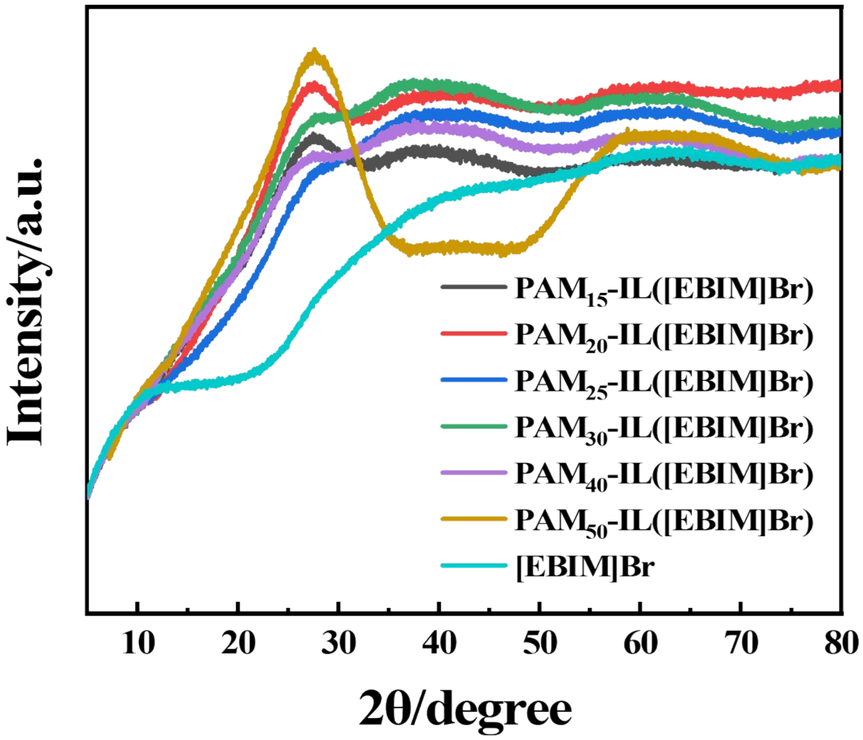

Figure S6. The XRD spectra of PAM_x-IL([EBIM]Br) ionogels and [EBIM]Br ionic liquid.

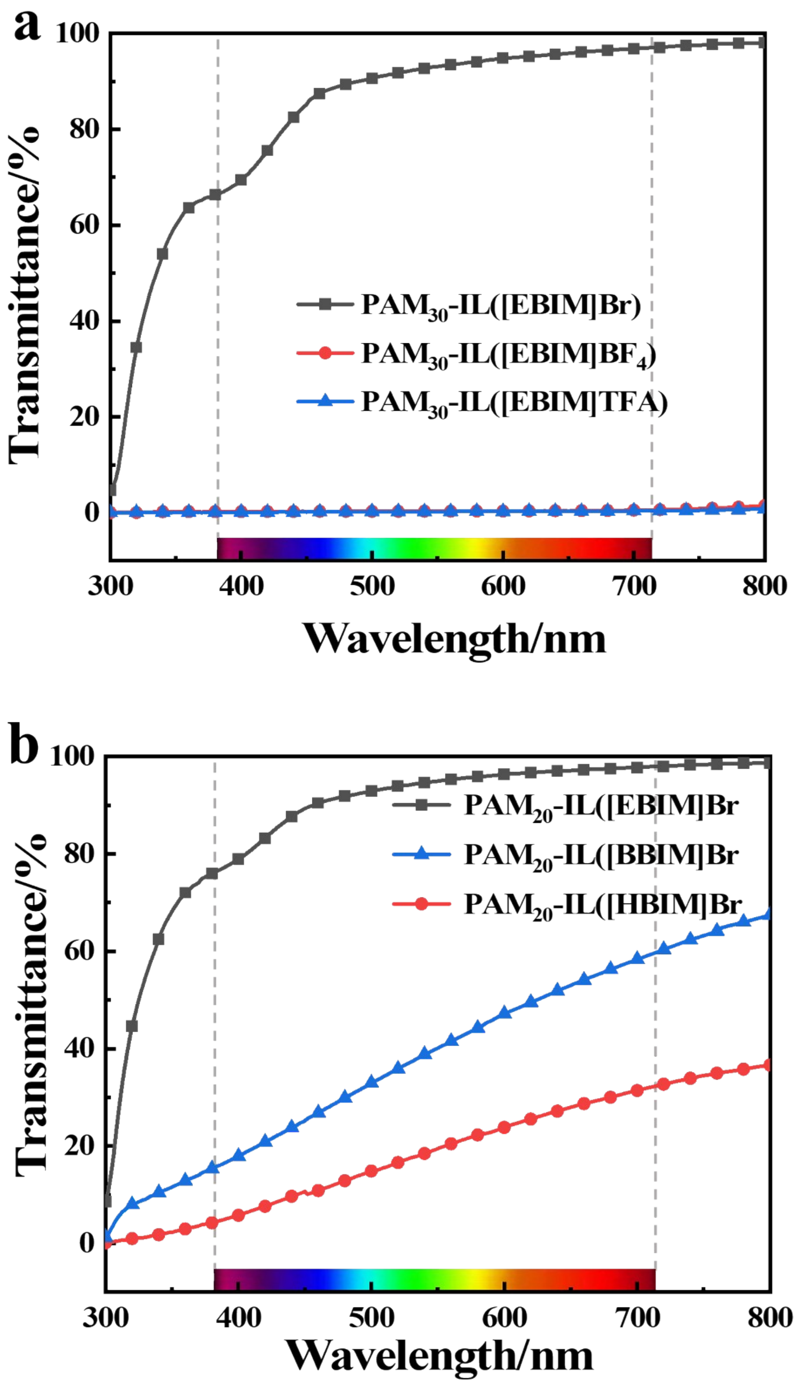

Figure S7. (a, b) Visible light transmittance spectra of (a) PAM_{30}-IL(Y) ionogels, Y=[EBIM]Br, [EBIM]BF_4, and [EBIM]TFA, (b) PAM_{20}-IL(Y) ionogels, Y=[EBIM]Br, [BBIM]Br, and [HBIM]Br.

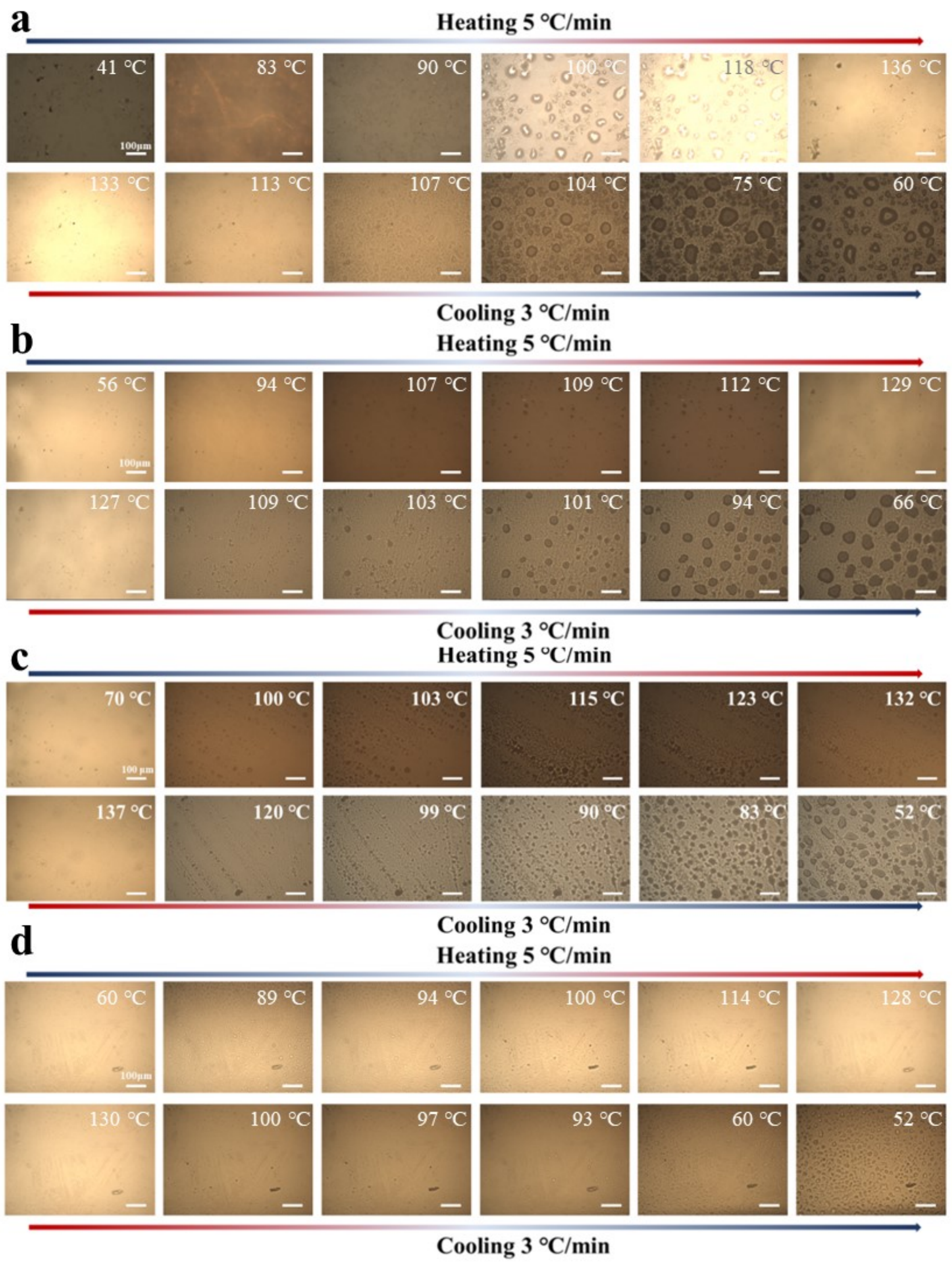

Figure S8. Phase separation process of (a) PAM_{30}-IL([EBIM]Br) ionogel, (b) PAM_{35}-IL([EBIM]Br) ionogel, (c) PAM_{40}-IL([EBIM]Br) ionogel and (d) PAM_{50}-IL([EBIM]Br) ionogel during temperature rise (from RT to 140 ℃, 5℃/min) and fall (from 140℃ to RT, 5℃/min) observed by optical microscope.

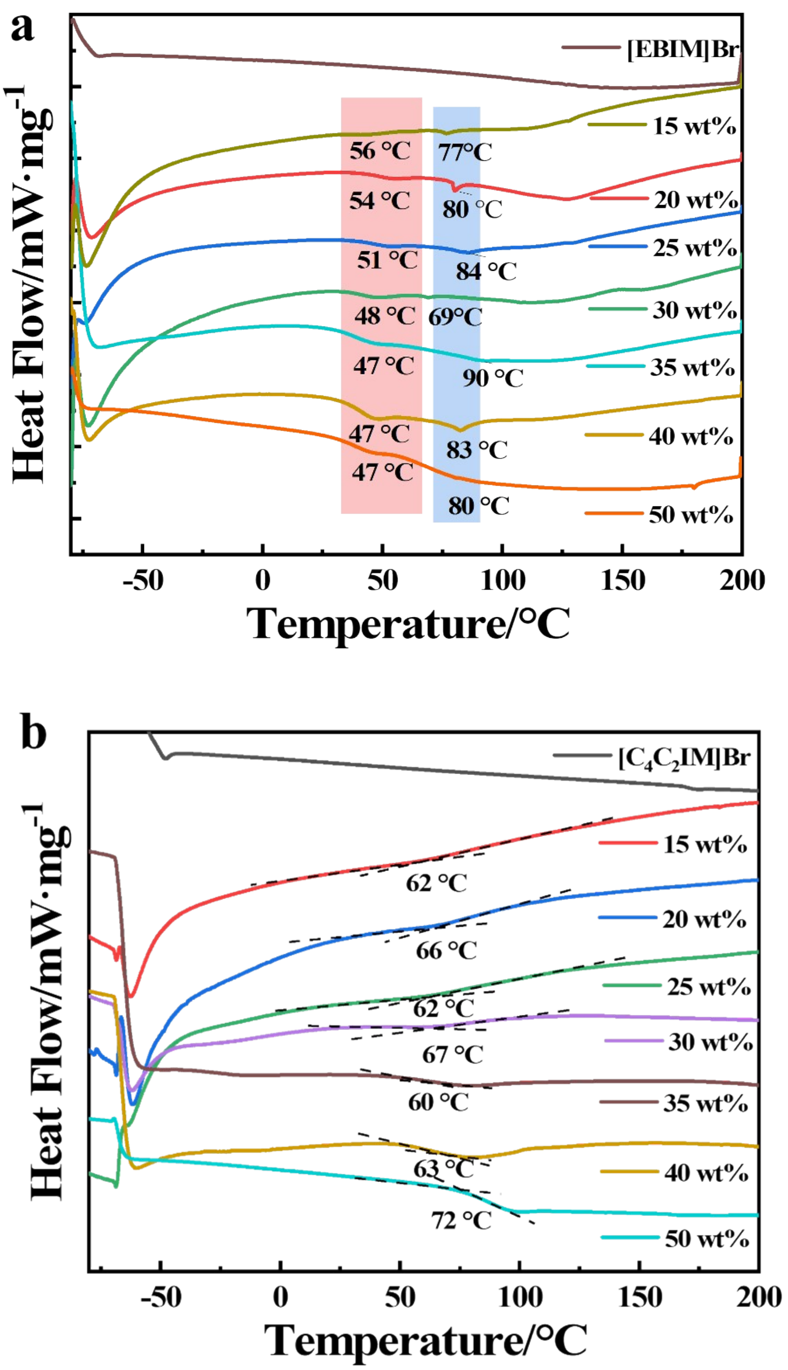

Figure S9. DSC curves of (a) PAM_x-IL([EBIM]Br) ionogels, and (b) PAM_x-IL([EBIM]Br) ionogels after a cycle of heating up and down, the cooling rate is 10K/min.

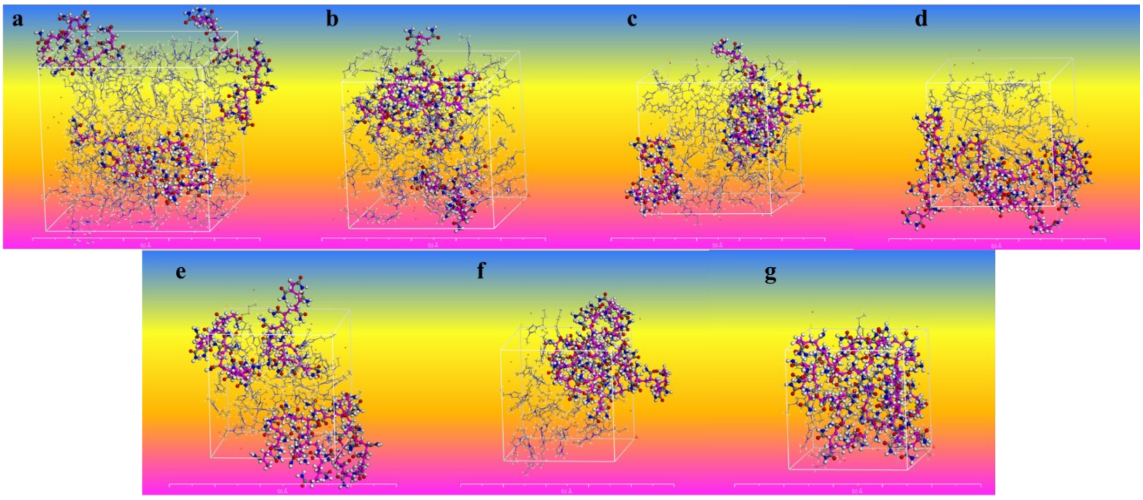

Figure S10. Structure models of PAM_x-IL([EBIM]Br) ionogels with anneal and dynamic optimized based on MD calculation, (a) PAM_{15}-IL([EBIM]Br) ionogel, (b) PAM_{20}-IL([EBIM]Br) ionogel, (c) PAM_{25}-IL([EBIM]Br) ionogel, (d) PAM_{30}-IL([EBIM]Br) ionogel, (e) PAM_{35}-IL([EBIM]Br) ionogel, (f) PAM_{40}-IL([EBIM]Br) ionogel, (g) PAM_{50}-IL([EBIM]Br) ionogel.

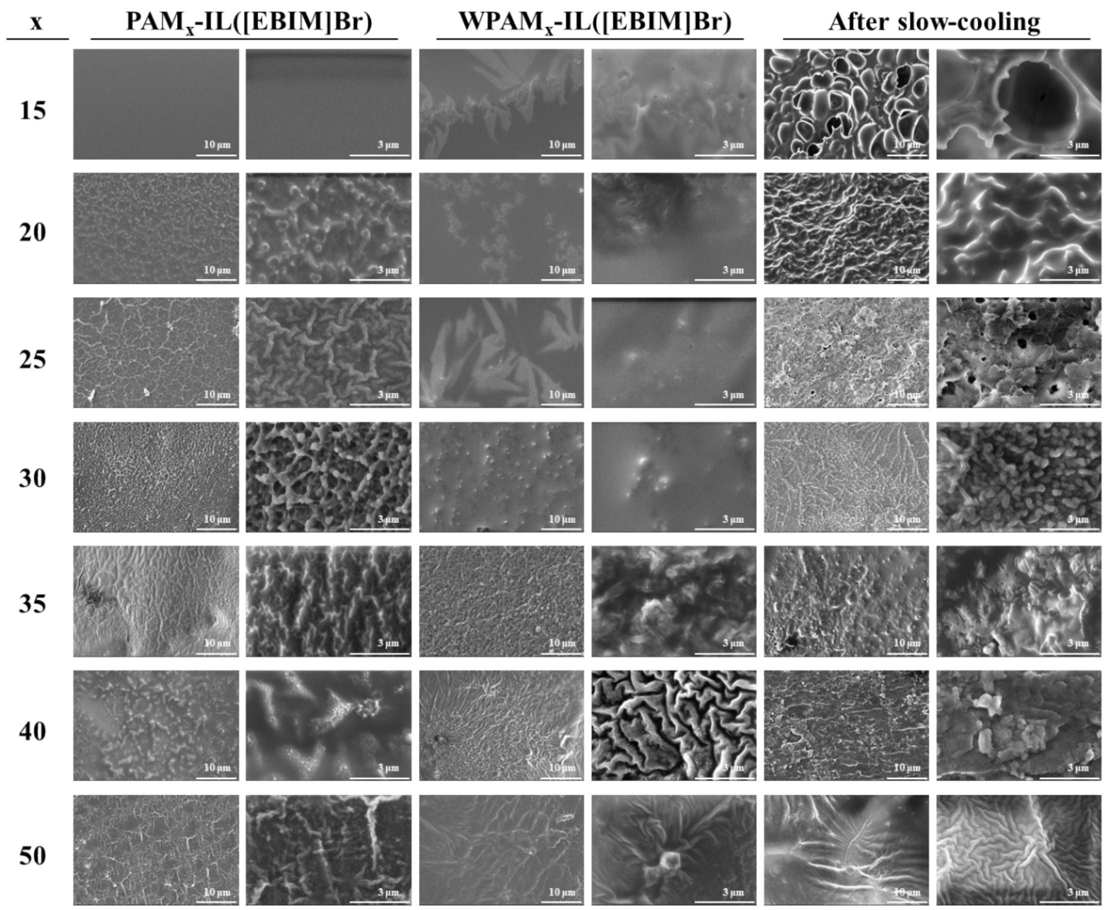

Figure S11. The SEM images of the phase separation structure of PAM_x-IL([EBIM]Br) ionogels, $WPAM_x$-IL([EBIM]Br) ionogels, and the corresponding ionogels obtained after slow cooling. The polymer content of the ionogels in each row is "x," where "x" represents the mass fraction of polymer (x=15, 20, 25, 30, 35, 40, or 50). The images on the right side of each column are magnifications of the corresponding images on the left side.

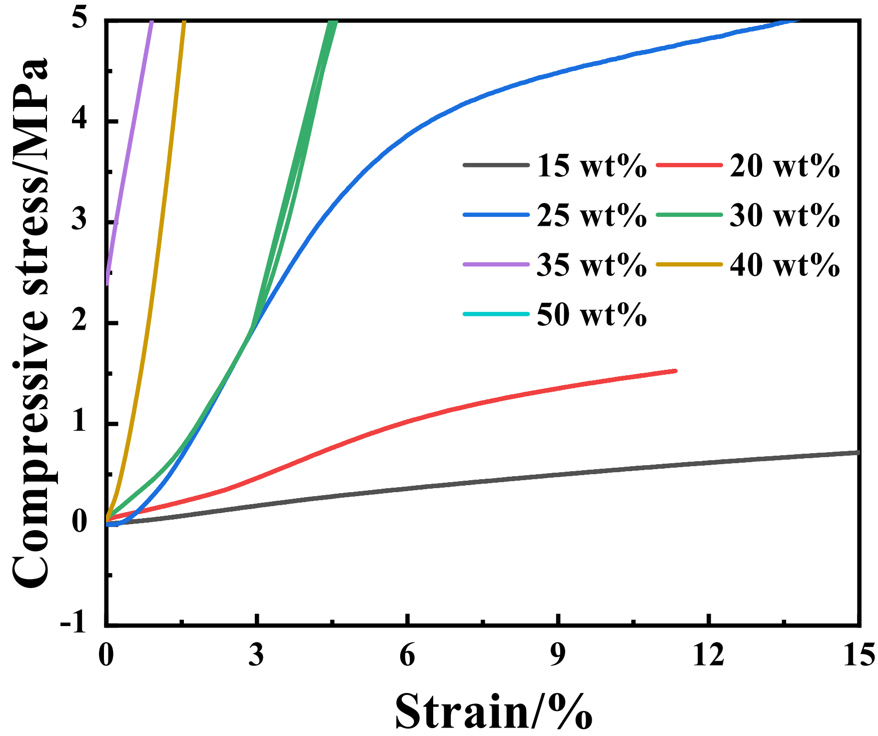

Figure S12. Compressive stress-strain curves of PAMx-IL([EBIM]Br) ionogels (magnification of the black dashed area in Figure 3c).

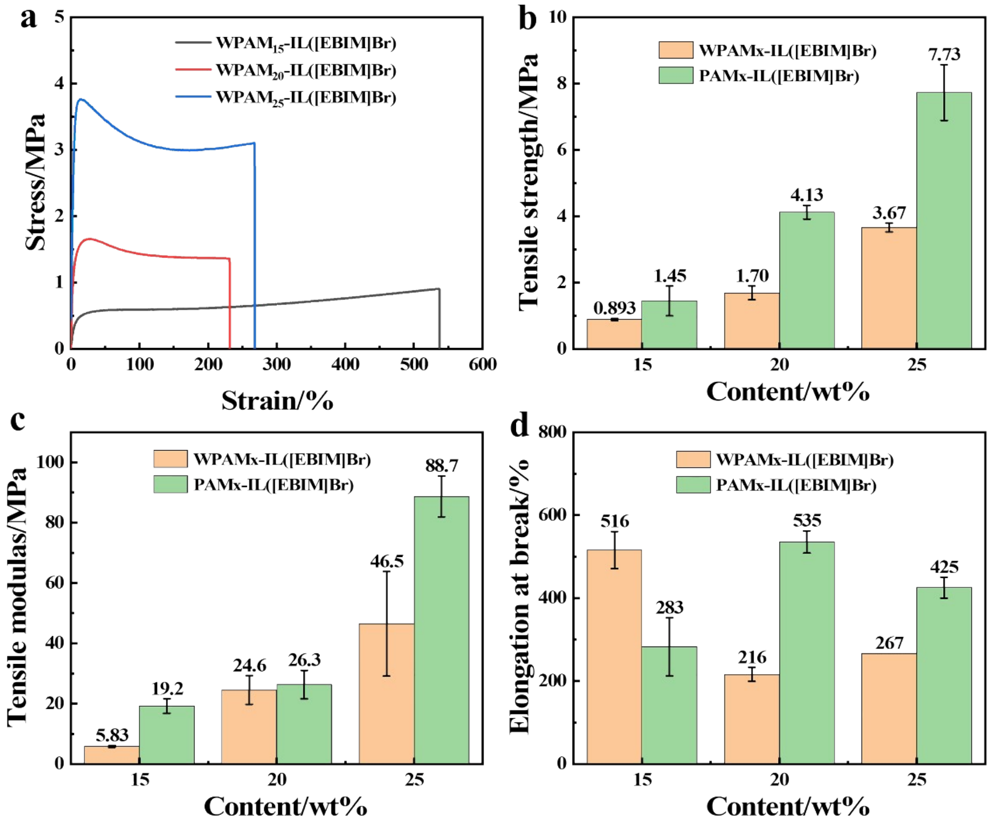

Figure S13. Mechanical properties of WPAM$_x$-IL([EBIM]Br) ionogels. (a) Tensile stress-strain curves of WPAM$_x$-IL([EBIM]Br). (b-d) A comparison between WPAM$_x$-IL([EBIM]Br) and PAM$_x$-IL([EBIM]Br) in relation to (b) tensile strength, (c) tensile modulus, and (d) elongation at break. x=15, 20 and 30. Error bars show standard deviation from three independent samples.

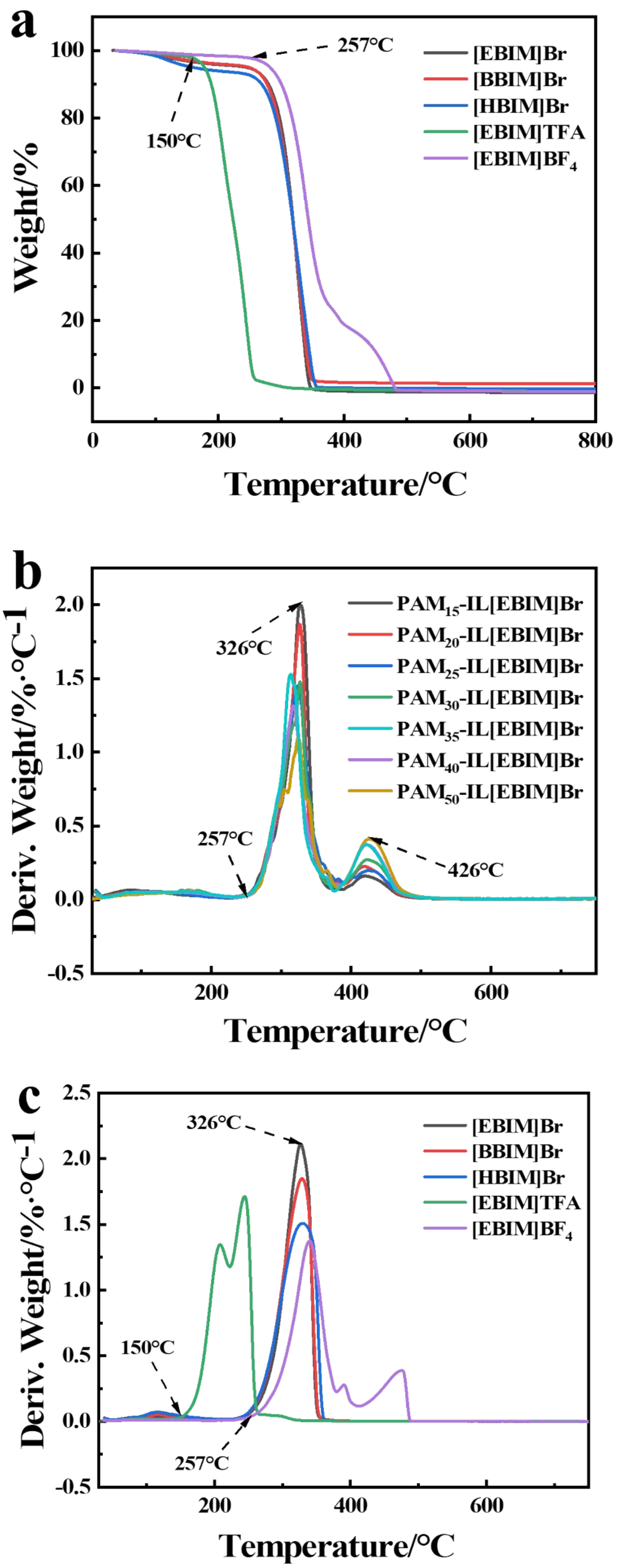

Figure S14. (a) TGA curves of ionic liquids, (b) DTG curves of PAM_x-IL([EBIM]Br) ionogels, and (c) DTG curves of ionic liquids.

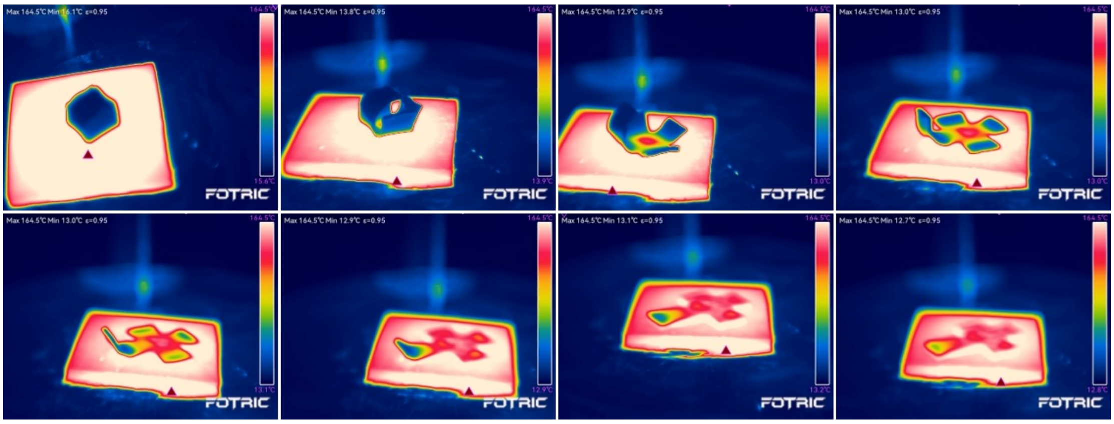

Figure S15. Infrared thermal imaging photos of thermally driven shape-memory behavior of PAM40-IL ionogel programmed as box shape.

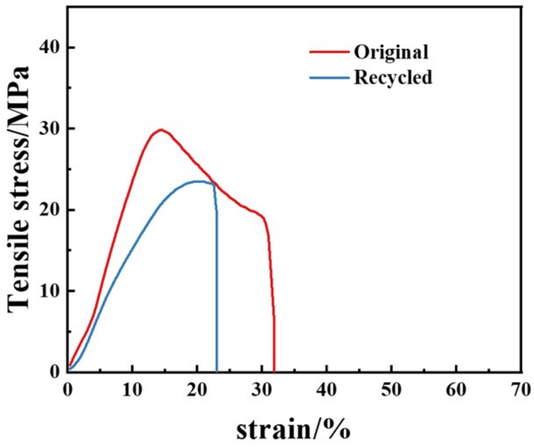

Figure S16. The mechanical properties of PAM_{40}-IL([EBIM]Br) ionogel before and after recycling.

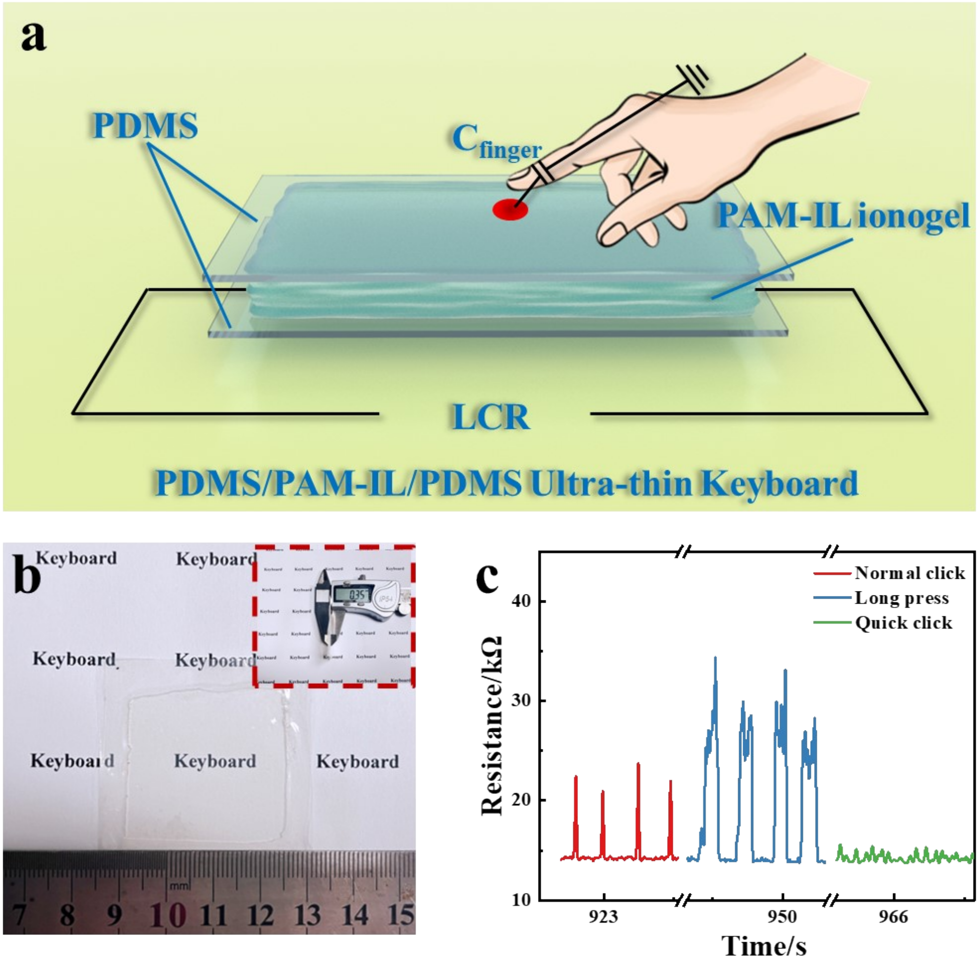

Figure S17. PDMS/PAM-IL/PDMS ultra-thin keyboard. (a) Schematic diagram, (b) Optical photograph, (c) Signal curves under different click modes.

Table S1. Performance summary of PAM_x-IL(Y) ionogels.

Ionogel	Transmittance /%	Density /g·cm^{-3}	Tensile strength /MPa	Tensile modulus /MPa	Elongation at break /%	Tensile yield strength /MPa	Conductivity /S·cm^{-1}	Compressive strength /MPa	Compressive modulus /MPa	Thermal decomposition temperature/°C
PAM_{15}-IL([EBIM]Br)	94.0	1.267	1.45	19.2	283	1.08	0.875	0.30	7.0	257
PAM_{20}-IL([EBIM]Br)	98.6	1.273	4.13	26.3	535	1.66	0.920	0.95	17.1	257
PAM_{25}-IL([EBIM]Br)	95.7	1.271	7.73	88.7	425	4.70	0.542	3.9	85.3	257
PAM_{30}-IL([EBIM]Br)	98.0	1.282	10.4	143.18	386.7	8.45	0.849	10.1	201.1	257
PAM_{35}-IL([EBIM]Br)	91.8	1.290	19.1	251.6	229	19.5	0.036	17.1	334.2	257
PAM_{40}-IL([EBIM]Br)	92.2	1.300	31.1	319.80	30.2	29.8	0.042	36.6	683.3	257
PAM_{50}-IL([EBIM]Br)	96.7	1.308	Too hard and brittle to test				0.023	112.2	1771.8	257
PAM_{20}-IL([BBIM]Br)	66.6	1.209	Too brittle to test							
PAM_{20}-IL([HBIM]Br)	36.3	1.164	Too brittle to test							
PAM_{30}-IL([EBIM]BF_4)	1.39	1.255	Obvious leakage, too brittle to test							
PAM_{30}-IL([EBIM]TFA)	0.76	1.254	Obvious leakage, too brittle to test							

Table S2. The mechanical properties of $WPAM_x$-IL([EBIM]Br) and PAM_x-IL([EBIM]Br) ionogels.

Ionogel	Tensile strength/MPa	Tensile modulus/MPa	Elongation at break/%	tensile Yield strength/MPa
PAM_{15}-IL([EBIM]Br)	1.45	19.2	283	1.08
PAM_{20}-IL([EBIM]Br)	4.13	26.3	535	1.66
PAM_{25}-IL([EBIM]Br)	7.73	88.7	425	4.70
$WPAM_{15}$-IL([EBIM]Br)	0.91	5.83	536	0.51
$WPAM_{20}$-IL([EBIM]Br)	1.65	24.6	231	1.65
$WPAM_{25}$-IL([EBIM]Br)	3.76	46.5	267	3.76

Table S3. The mechanical properties of reported high strength gel materials.

No.	Strength/MPa	Modulus/MPa	Toughness/MJ·m^{-3}	Type
1	3.64	0.46	27.60	Hydrogel[1]
2	5.60	1.30	--	Hydrogel[2]
3	3.10	0.60	8.65	Hydrogel[3]
4	1.36	0.49	--	Hydrogel[4]
5	2.00	--	22.00	Hydrogel[5]
6	2.70	1.17	10.80	Hydrogel[6]
7	2.20	0.27	--	Hydrogel[7]
8	2.70	0.82	8.50	Hydrogel[8]
9	9.30	277.00	0.40	Hydrogel[9]
10	20.20	16.10	62.70	DES gel[10]
11	5.19	0.20	--	PU-IL ionogel[11]
12	2.52	1.43	2.55	PU-IL ionogel[12]
13	22.00	--	109.80	PU-IL ionogel[13]
14	4.99	1.71	--	PU-IL ionogel[14]
15	9.15	1.12	178.46	BC ionogel[15]
16	300.00	5000.00	16.00	BC ionogel[16]
17	3.70	2.46	6.25	Organic-inorganic ionogel[17]
18	0.23	0.04	--	PILs ionogel[18]
19	2.28	2.28	--	PILs ionogel[19]
20	15.00	82.81	--	PILs ionogel[20]
21	12.60	46.50	--	P(AA-co-AM) ionogel[21]
22	7.12	0.94	--	P(IBA-co-MEA) ionogel[22]
23	0.37	0.42	21.80	PAA/CNF ionogel[23]
24	14.30	55.00	78.00	PDMAA ionogel[24]
25	0.90	15.60	2.48	PSHM ionogel[25]
26	4.80	0.48	--	PEA ionogel[26]
27	7.60	58.00	25.00	PDMAA/MOF ionogel[27]
This work	**31.10**	**319.80**	**32.90**	**PAM-IL ionogel**

Reference

1. N. Yuan, L. Xu, H. Wang, Y. Fu, Z. Zhang, L. Liu, C. Wang, J. Zhao and J. Rong, ACS Appl. Mater. Inter., 2016, 8, 34034.
2. Y. Yang, X. Wang, F. Yang, L. Wang and D. Wu, Adv. Mater., 2018, 30, 1707071.
3. S. X. Pan, M. Xia, H. H. Li, X. L. Jiang, P. X. He, Z. G. Sun and Y. H. Zhang, J. Mater. Chem. C, 2020, 8, 2827.
4. S. H. Li, H. Y. Pan, Y. T. Wang and J. Q. Sun, J. Mater. Chem. A, 2020, 8, 3667.
5. T. Nakajima, Y. Fukuda, T. Kurokawa, T. Sakai, U. I. Chung and J. P. Gong, ACS Macro Lett., 2013, 2, 518.
6. L. J. Zhou, X. J. Pei, K. Fang, R. Zhang and J. Fu, Polymer, 2020, 192, 122319.
7. J. Wen, X. Zhang, M. Pan, J. Yuan, Z. Jia and L. Zhu, Polymers, 2020, 12, 239.
8. Y. Zhang, M. Y. Li, X. Han, Z. W. Fan, H. H. Zhang and Q. L. Li, Chem. Phys. Lett., 2021, 769, 138437.
9. H. P. Yu and Y. J. Zhu, Nano Research, 2021, 14, 3643.
10. H. Zhang, N. Tang, X. Yu, M. H. Li and J. Hu, Adv. Funct. Mater., 2022, 32, 2206305.
11. M. W. Zhang, R. Yu, X. L. Tao, Y. Y. He, X. P. Li, F. Tian, X. Y. Chen and W. Huang, *Adv. Funct. Mater.*, 2022, **33**, 2208083.
12. T. Li, Y. Wang, S. Li, X. Liu and J. Sun, Adv. Mater., 2020, 32, 2002706.
13. P. Liu, D. F. Pei, Y. P. Wu, M. J. Li, X. H. Zhao and C. X. Li, J. Mater. Chem. A, 2022, 10, 25602.
14. H. Wang, J. Xu, K. Li, Y. Dong, Z. Du and S. Wang, J. Mater. Chem. B, 2022, 10, 1301.
15. G. D. Fan, K. K. Liu, H. Su, Y. Q. Luo, Y. Geng, L. Y. Chen, B. J. Wang, Z. P. Mao, X. F. Sui and X. L. Feng, Chem. Eng. J., 2022, 434, 134702.
16. W. Choi, A. Abraham, J. Ko, J. G. Son, J. Cho, B. I. Sang and B. Yeom, ACS Appl. Mater. Inter., 2022, 14, 30056.
17. L. Yu, S. Guo, Y. Lu, Y. Li, X. Lan, D. Wu, R. Li, S. Wu and X. Hu, Adv. Energy Mater., 2019, 9, 1900257.
18. Y. Zhao, D. L. Gan, L. C. Wang, S. Y. Wang, W. J. Wang, Q. Wang, J. J. Shao and X. C. Dong, Adv. Mater. Tech., 2023, 8, 2201566.
20. Z. Yu and P. Wu, Adv. Mater., 2021, 33, 2008479.
21. M. Wang, P. Zhang, M. Shamsi, J. L. Thelen, W. Qian, V. K. Truong, J. Ma, J. Hu and M. D. Dickey, Nat. Mater., 2022, 21, 359.
22. B. Yiming, Y. Han, Z. Han, X. Zhang, Y. Li, W. Lian, M. Zhang, J. Yin, T. Sun, Z. Wu, T. Li, J. Fu, Z. Jia and S. Qu, Adv. Mater., 2021, 33, 2006111.
23. Y. H. Ye, H. Oguzlu, J. Y. Zhu, P. H. Zhu, P. Yang, Y. L. Zhu, Z. M. Wan, O. J. Rojas and F. Jiang, Adv. Funct. Mater., 2023, 33, 2209787.
24. L. Li, W. Li, X. Wang, X. Zou, S. Zheng, Z. Liu, Q. Li, Q. Xia and F. Yan, Angew. Chem. Int. Ed. Engl., 2022, 61, 202212512.
25. K. G. Cho, S. An, D. H. Cho, J. H. Kim, J. Nam, M. Kim and K. H. Lee, Adv. Funct. Mater., 2021, 31, 2102386.
26. Z. Q. Cao, H. L. Liu and L. Jiang, Mater. Horiz., 2020, 7, 912.
27. Q. Xia, W. Li, X. Zou, S. Zheng, Z. Liu, L. Li, F. Yan, Mater. Horiz., 2022,9, 2881.